Comparative solution equilibrium studies of anticancer gallium(III) complexes of 8-hydroxyquinoline and hydroxy(thio)pyrone ligands

Éva A. Enyedy[a*], Orsolya Dömötör[a], Erika Varga[a], Tamás Kiss[a,b], Robert Trondl[c], Christian G. Hartinger[c,d], Bernhard B. Keppler[c,e]

[a]Department of Inorganic and Analytical Chemistry, University of Szeged, Dóm tér 7. H-6720 Szeged, Hungary

[b]Bioinorganic Chemistry Research Group of the Hungarian Academy of Sciences, University of Szeged, Dóm tér 7. H-6720 Szeged, Hungary

[c]Institute of Inorganic Chemistry, University of Vienna, Waehringer Str. 42, A-1090 Vienna, Austria

[d]School of Chemical Sciences, The University of Auckland, PB: 92019, 1142 Auckland, New Zealand

[e]University of Vienna, Research Platform Translational Cancer Therapy Research, Waehringer Str. 42, A-1090 Vienna, Austria

Keywords: Stability Constants, Gallium Antitumor Complexes, Oxine, Maltol, Thiomaltol, Fluorescence

* Corresponding author: E-mail: enyedy@chem.u-szeged.hu (É.A. Enyedy); Fax: +36 62 420505

ABSTRACT

The stoichiometry and stability constants of the Ga(III) complexes of 8-hydroxyquinoline (HQ), 8-hydroxyquinoline-5-sulfonate (HQS), maltol, thiomaltol, allomaltol and thioallomaltol were determined by means of pH-potentiometry, UV-Vis spectrophotometry, spectrofluorimetry and ^{1}H NMR spectroscopy in aqueous solution. Spectrofluorimetry was used to determine the stability constants of the Ga(III)-HQ species in water. Formation of $[GaL]^{2+}$, $[GaL_2]^{+}$ and $[GaL_3]$ complexes was found and the Ga(III) binding ability of the ligands followed the order: thioallomaltol < thiomaltol < allomaltol < maltol << HQS ~ HQ. As a result of the outstanding stability of *tris*(8-hydroxyquinolinato)gallium(III) (KP46) the dissociation of the complex is negligible at physiological pH even in the biologically relevant low concentration range. Thus KP46 is able to preserve its original entity more considerably than other Ga(III) complexes. Moreover, intrinsic fluorescence of KP46 allows the monitoring of the cellular accumulation and distribution in human cancer cells by fluorescence microscopy.

1. Introduction

Numerous gallium(III) complexes inhibit tumor growth and Ga was the second metal ion, after platinum to be administered to cancer patients in various clinical trials [1-4]. Ga is used in a wide variety of applications, such as medical imaging for some cancer types, infections and inflammatory diseases in form of ^{67}Ga(III) and ^{68}Ga(III) radiopharmaceuticals [5] and fluorescent Ga(III) compounds possibly in organic light-emitting diodes [6]. Remarkably, the simple salt Ga(III) nitrate exerts antineoplastic effects in particular for the treatment of lymphoma and bladder cancer and has a therapeutic effect in cancer-related hypercalcaemia (Ganite^{TM} in clinical use) [3]. Orally administered Ga(III) salts are not sufficiently bioavailable. A prolonged exposure of low steady-state Ga(III) concentration in the blood can result in an improved therapeutic index, that can be assured by application of charge neutral Ga(III) complexes [4]. Accordingly, many compounds have been prepared and tested by *in vitro* and *in vivo* studies. Promising compounds are found to be the six-coordinate *tris*-ligand Ga(III) complexes and *tris*(3-hydroxy-2-methyl-4H-pyran-4-onato)Ga(III) (Ga-maltolate) and *tris*(8-quinolinolato)Ga(III) (KP46) are in clinical trials [1,2]. Both complexes can be administered orally, exhibit moderate side effects and can overcome Ga(III) nitrate resistance [3,7,8].

The supposed mode of action of these Ga(III) complexes corresponds to the similarity of Ga(III) to Fe(III) in terms of charge, ionic radius, electronegativity, electron affinity and coordination geometry. However, Ga(III) is redox inactive, thus it can interfere with the cellular iron metabolism but cannot participate in biologically important redox processes. The primary target is supposed to be the iron-containing ribonucleotide reductase, the rate determining enzyme in the supply of deoxyribonucleotides for DNA synthesis required for cell proliferation. Binding of Ga(III) to the iron site of the R2 subunit of this enzyme results in the destabilization of the tyrosyl radical essential for enzymatic activity [9]. Ga(III) is able to

bind to the iron sites of transferrin, which promotes the cellular absorption of Ga(III) [10], in particular in proliferating cancer cells with strong iron demand and overexpressed transferrin receptors, although cellular gallium uptake may also occur by a transferrin-independent pathway [5,9].

The actual chemical forms of the active antitumor Ga(III) complexes may differ from the originally administered ones depending on their stability in aqueous solution and tendency to interact with endogenous bioligands which show strong Ga(III) binding ability such as human serum transferrin. Consequently, in order to better understand the pharmacokinetic and biodistribution profile of these metal complexes the knowledge of the speciation and the most plausible chemical forms in aqueous solution, especially at physiological pH, is a mandatory prerequisite. However, so far no stability constants are available in the literature for the Ga(III) complexes of 8-hydroxyquinoline (HQ) and 3-hydroxy-2-methyl-4H-pyran-4-one (maltol) complexes in water (Chart 1). The poor water-solubility of neutral KP46, which is advantageous for the improved intestinal absorption [1,11], limits the applicability of traditional methods such as pH-potentiometry. Therefore, we performed detailed pH-potentiometric, UV-Vis spectrophotometric, ^{1}H NMR spectroscopic and spectrofluorimetric measurements to investigate the stoichiometry and stability of the Ga(III) complexes of HQ, maltol and some of their derivatives in water and water/dimethyl sulfoxide (DMSO) mixtures.

2. Experimental

2.1. Chemicals

Maltol, HQ and HQS were purchased from Sigma-Aldrich and used without further purification. Allomaltol, thiomaltol and thioallomaltol were prepared according to literature procedures [12,13]. The purity and stability of the ligands were checked and the exact concentrations of the stock solutions were determined by the Gran method [14]. $GaCl_3$ and

$Ga(NO_3)_3$ stock solutions were prepared in HCl and HNO_3, respectively. Their concentrations were determined by complexometry via the EDTA complexes. Accurate strong acid content of the metal stock solutions was determined by pH-potentiometric titrations.

2.2. pH-Potentiometric studies

The pH-potentiometric measurements for the determination of the protonation constants of the ligands and of the overall stability constants of the Ga(III) complexes of hydroxy(thio)pyrones and HQS were carried out at 25.0 ± 0.1 °C in water at an ionic strength of 0.20 M (KCl, Sigma-Aldrich) and in DMSO:water 30:70 and 60:40 (w/w) as solvents (for the complexes of maltol, HQ and HQS) and at an ionic strength of 0.10 M KCl in order to keep the activity coefficients constant. The Ga(III)−maltol complexes were also studied at 25.0 ± 0.1 °C in water at an ionic strength of 0.20 M (KNO_3, Sigma-Aldrich). The titrations were performed with carbonate-free KOH solution of known concentration (0.20 M for measurements in water and 0.10 M for samples containing DMSO). KOH, HCl and HNO_3 were Sigma-Aldrich products and their concentrations were determined by pH-potentiometric titrations. An Orion 710A pH-meter equipped with a Metrohm combined electrode (type 6.0234.100) and a Metrohm 665 Dosimat burette were used for the pH-metric measurements. The electrode system was calibrated to the $pH = -\log[H^+]$ scale in water and in the DMSO/water solvent mixtures by means of blank titrations (strong acid *vs.* strong base; HCl *vs.* KOH), similarly to the method suggested by Irving *et al.* [15] in pure aqueous solutions. The average water ionization constant, pK_w, is 13.76 ± 0.01 in water, 14.53 ± 0.05 in DMSO:water 30:70 (w/w) and 16.15 ± 0.05 in DMSO:water 60:40 (w/w) at 25 °C, which corresponds well to literature data [16]. The reproducibility of the titration points included in the calculations was within 0.005 pH units. The pH-metric titrations were performed in the pH range 2.0–11.5 for water, 2.0–12.5 for DMSO:water 30:70 (w/w) and 2.0–13.8 for

DMSO:water 60:40 (w/w). The initial volume of the samples was 10.0 or 5.0 mL. The ligand concentration was in the range 0.8–4 mM and metal ion-to-ligand ratios of 1:1 to 1:8 were used. The fitting of the titration curves was less than 0.01 mL. (The fitting parameter is the average difference between the experimental and calculated titration curves expressed in the volume of the titrant.) Samples were deoxygenated by bubbling purified argon through them for *ca.* 10 min prior the measurements.

The protonation constants of the ligands were determined with the computer program HYPERQUAD [17]; PSEQUAD [18] was utilized to establish the stoichiometry of the complexes and to calculate the stability constants (log $\beta(M_pL_qH_r)$) employing literature data for Ga(III) hydroxido complexes [19]. $\beta(M_pL_qH_r)$ is defined for the general equilibrium pM + qL + rH $\rightleftharpoons$ $M_pL_qH_r$ as $\beta(M_pL_qH_r) = [M_pL_qH_r]/[M]^p[L]^q[H]^r$ where M denotes the metal ion and L the deprotonated ligand. The calculations were always made from the experimental titration data measured in the absence of any precipitate in the solution.

2.3. Spectrophotometric, spectrofluorimetric and ^{1}H NMR measurements

A Hewlett Packard 8452A diode array spectrophotometer was used to record the UV-visible (UV-Vis) spectra in the interval 200–800 nm. The path length was 1 cm for samples containing hydroxy(thio)pyrones or HQS and 2 cm for samples containing HQ. Protonation and stability constants and the individual spectra of the species were calculated with the computer program PSEQUAD [18]. The spectrophotometric titrations were performed on samples of the ligands with or without Ga(III); the concentration of the ligands was 0.10 mM and 0.05 mM in case of the hydroxythiopyrones and HQ). The metal-to-ligand ratios were 1:1, 1:2, 1:3 over the pH range used in pH-potentiometric measurements at 25.0 ± 0.1 °C at an ionic strength of 0.20 M (KCl) in pure water or of 0.10 M (KCl) in DMSO/water mixtures. Measurements for 1:1 ligand–to-Ga(III) systems were also carried out in these solvent

systems by preparing individual samples in which KCl was partially or completely replaced by HCl and pH values, varying in the range *ca.* 1.0–2.0, were calculated from the HCl content. In the case of maltol, individual samples were also prepared in which KCl and HCl were replaced with KNO_3 and HNO_3, applying 0.20 M ionic strength in the pH range 1.0–2.0.

The pH-dependent fluorescence measurements were carried out on a Hitachi-4500 spectrofluorimeter with the excitation at 367 nm for HQ containing samples. The emission spectra were recorded in 1 cm quartz cell in the pH range between 2 and 11.5 in water at 25.0 ± 0.1 °C using 10 nm/10 nm slit widths. The samples contained 0.05 mM HQ at 0.20 M (KCl) ionic strength and the metal-to-ligand ratios were varied (1:1, 1:2, 1:3, 1:5). Proton dissociation and stability constants were calculated with the computer program PSEQUAD [18]. Three-dimensional spectra were recorded in the 210–550 nm excitation and 220–650 nm emission wavelength regions for the Ga(III)–HQ (1:3) system at pH 7.4.

^{1}H NMR spectroscopic studies were carried out on a Bruker Ultrashield 500 Plus instrument. Hydroxythiopyrones and hydroxypyrones were dissolved in a 10% D_2O/H_2O mixture to yield a concentration of 0.5 and 3.0 mM, respectively. The Ga(III)-to-ligand ratio was 1:3 at 0.20 M (KCl) ionic strength at 25.0 °C and spectra were recorded in the range 25−65 °C in a temperature-dependence study of the Ga(III)–thiomaltol system. In the case of the hydroxythiopyrones samples were deoxygenated by bubbling argon through them for about 10 min before the measurements.

2.4. Determination of the distribution and partition coefficients

The octanol/water distribution coefficients (log*D*) of allomaltol, thiomaltol, thioallomaltol were determined by the shake-flask method [20] in *n*-octanol/water solutions at 25.0 ± 0.2 ^{o}C {at pH 2.0 (HCl) or 7.40 (4-(2-hydroxyethyl)-1-piperazineethanesulfonic acid, HEPES}. All ligands (40 μM) were dissolved in the *n*-octanol pre-saturated aqueous solution

(0.01 M HEPES or HCl) containing KCl (0.20 M). After shaking the aqueous solutions and *n*-octanol with 1:1 phase ratio for 2 h, the mixtures were centrifuged at 4000 rpm for 15 min by a temperature controlled centrifuge (Sanyo). Two parallel experiments were performed for each sample. After the separation of the two phases, the pH values of the aqueous solution were controlled to be within ± 0.02 units to those of the starting solution. UV-visible (UV-Vis) spectra of the ligands in the aqueous phase were compared with those of the starting aqueous solutions in the range 260–450 nm. *D* was calculated as the mean of (Absorbance$_{original}$ / Absorbance$_{aqueous\ phase}$ − 1) obtained at λ_{max} ± 10 nm. *D* always represents the ratio of concentrations of all species (ionized and neutral) in the organic and aqueous phases, therefore is pH-dependent, while the pH-independent partition coefficient (*P*) is related to the neutral, non-ionized species which are transferred into the organic phase, thus *P* shows the equilibrium concentration ratio of the solute between the two phases [20,21]. Calculation of the *D* and *P* values of the ligands is based on the following equations [21]:

$$HL_{aq} \rightleftharpoons L^-_{aq} + H^+_{aq} \qquad K_a = \frac{[L^-]_{aq}[H^+]_{aq}}{[HL]_{aq}} \qquad (1)$$

$$c_{HL} = [HL]_{aq} + [L^-]_{aq} + [HL]_{n\text{-octanol}} \qquad (2)$$

$$D = \frac{[HL]_{n\text{-octanol}}}{[HL]_{aq} \times (1 + \frac{K_a}{[H^+]})} = \frac{P}{(1 + \frac{K_a}{[H^+]})} \qquad (3)$$

$$P = D \times (1 + K_a/[H^+]) \qquad (4)$$

2.5. Cell culture conditions and fluorescence microscopy

SW480 cells (colon carcinoma, human) were purchased from the American Type Culture Collection (ATCC). Cells were grown in Eagle's Minimal Essential Medium (MEM) supplemented with heat-inactivated 10% fetal bovine serum, 1 mM sodium pyruvate, 4 mM L-glutamine, and 1% nonessential amino acids in a humidified incubator at 37 °C and 5%

CO_2. Cells were seeded on cover slips in 6-well plates 24 h prior to treatment. The Ga(III)-HQ (1:3) working solution for fluorescence microscopy was prepared from a DMSO stock solution and was diluted in MEM supplied with 10% fetal calf serum. No precipitation of the compound was observed in the working solution under this condition. Cells were exposed to 150 and 300 μM Ga(III)–HQ (1:3) for 5 min, 30 min, 1 and 3 h, washed with phosphate buffered saline (PBS) and imaging was done using a fluorescence microscope BX40, an U-MWU filter cube, an F-View CCD Camera (all Olympus), Cell-F fluorescence imaging software (Olympus) and a 60× magnification oil immersion objective lens.

3. Results and discussion

3.1. Proton dissociation processes and lipophilicity of the ligands

The proton dissociation constants of the hydroxypyrone (maltol, allomaltol) and hydroxythiopyrone (thiomaltol, thioallomaltol) derivatives (see Chart 1) were determined by pH-potentiometric and UV-Vis spectrophotometric titrations in pure aqueous solution (Table 1).

Table 1

pK_a Values of these ligands have been reported with the exception of thioallomaltol [22-24], but identical conditions (25 °C, I = 0.20 M (KCl)) were only used for maltol [22]. The values determined are in a good agreement with the literature data. The proton dissociation constants can be attributed most probably to the deprotonation of the hydroxyl functional group and the process is accompanied by characteristic changes of the ligand bands in the UV-Vis spectra. The development of new strong bands with higher λ_{max} values was observed for all ligands due to the deprotonation (Fig. 1), which resulted in more extended conjugated π electron systems. In addition to the pK_a values, the individual UV-Vis spectra of the ligand species

(HL and L^-) were also calculated on the basis of deconvolution of the pH-dependent UV-Vis spectra (see Fig. 1 and Table 1). The thio derivatives tend to get oxidized (due to the thiol-thione tautomerism) under aerobic conditions especially when they are in their deprotonated forms. However, this could be avoided by recording the spectra under argon atmosphere and resulted in a constant location of the isosbestic points. Concentration distribution curves of allomaltol and thiomaltol calculated on the basis of the pK_a values, together with the absorbance values at the λ_{max} as a function of pH are shown in the insets of Fig. 1.

Fig. 1

The sulfur-containing derivatives possess ~0.4 log units lower pK_a values owing to the lower electronegativity and more polarizable nature of S, which provides a more increased electron delocalization in the aromatic ring and hence more stable conjugated bases of thiomaltol and thioallomatol as compared to the corresponding reference compounds. On the other hand the position of the methyl group has also a significant effect on the deprotonation, namely the allo derivatives have lower pK_a values. In these molecules the electron donating methyl group is situated at *para* position to the hydroxyl group and the shielding effect of the electron withdrawing oxygen atoms becomes less pronounced as compared to the *ortho* position.

The *n*-octanol-water partition coefficient (log*P*) of the allomaltol (see Table 1) was calculated from the distribution coefficient (log*D*) measured at pH 7.4 using the proton dissociation constant, while these values are known for the maltol [21]. Since thiopyrones can undergo oxidation under aerobic conditions in their deprotonated form (*vide supra*), their log*P* values were determined at pH 2.0, then log$D_{7.4}$ could be calculated. Note that partial oxidation of thiomaltol and thioallomaltol at pH 7.40 under aerobic conditions yielded strongly wavelength-dependent $D_{7.4}$ values when were measured directly. Lipophilicity data revealed higher lipophilicity of the thio ligands compared with the pyrone analogues as it is expected due to the nature of the sulfur atom as larger size and lower electronegativity. While the allo

derivatives are in general somewhat more hydrophilic as the ortho position of the methyl group to the hydroxyl moiety can result in a more compact compound which may bring weaker interactions with the solvent water molecules, thus higher log*P* values [25]. Note that the log*P* value of thiomaltol is higher than reported earlier [26], which is most probably related to analysis under inert atmosphere; while the value of allomaltol is also somewhat higher, though other kind of method was used for the determination [25].

The deprotonation processes of HQ and HQS (Chart 1) were followed by pH-potentiometry under various conditions, namely water and 30:70 and 60:40 DMSO/H_2O mixtures (see Table 2).

Table 2

The insufficient water solubility of the neutral Ga(III) complex of HQ does not allow performing the pH-potentiometric measurements in pure aqueous solutions; therefore, the complexation of HQ with Ga(III) could only be studied in a DMSO-water mixture by this method. For the sake of comparison, pK_a values of HQS and maltol were also determined in the 30% and 60% (w/w) DMSO/H_2O solvent mixtures. The sulfonic acid group of HQS is deprotonated in the whole pH range studied due to its strong acidic character. HQS and HQ feature the same coordination mode and HQS is considered as a model compound. It has a lower log*P* value due to the negatively charged sulfonate moiety (0.59 *vs.* 1.87) [27], which provides marked improvements in water solubility. pK_a Values in aqueous solutions are available in the literature for HQ and HQS but they were determined under somewhat different conditions [27−29]; however, our data gave similar constants. The first pK_a can presumably be mainly attributed to the deprotonation of the quinoline-NH^+, while pK_2 is largely attributed to the phenolic OH. Both the pK_a values of HQ are found to be higher compared to those of HQS due to the large electron-withdrawing effect of the sulfonate substituent. It is noteworthy that the pK_1 values of HQ and HQS are decreased, while the pK_2

constants and the pK_a of maltol are increased as the DMSO content of the solvent is elevated (see Table 2). The proton dissociation constants plotted against the reciprocal value of the relative permittivity (or dielectric constant, ε_r) of the solvent medium show linear dependence in all cases (Fig. S1). A positive slope is seen for the pK_a of maltol and pK_2 of HQ, HQS; while pK_1 values of HQ and HQS represent a negative slope. This phenomenon corresponds well to the expectations based on the Born electrostatic solvent model [30], namely the pK_a of cationic acids (quinoline-NH^+) is diminished, while that of the anionic bases (phenolic-OH) is increased in the presence of DMSO compared to pure water due to the isoelectronic and charge neutralization protonation processes, respectively.

The proton dissociation processes of HQ were also investigated in aqueous solution by UV-Vis spectrophotometry and by fluorimetric titrations because of the weak intrinsic fluorescence of the ligand. Two well-separated isosbestic points were observed at 334 and 320 nm (see Fig. 2) due to the deprotonation equilibria $H_2L^+ \rightleftharpoons HL + H^+$ and $HL \rightleftharpoons L^- + H^+$, respectively.

Fig. 2

The pK_1 value determined from the UV-Vis spectra of HQ is in a fairly good agreement to that obtained by pH-potentiometry (Table 2), however the values for pK_2 are slightly off. The fluorescence of HQ is quenched in the strongly acidic medium by the surrounding water molecules, but the deprotonation of the quinoline-NH^+ moiety results in an increase of the intensity and data were appropriate to accurately determine the first acidity constant (see Table 2 and Fig. S2). Parallel to the second deprotonation step the intensity decreased, but surprisingly at pH > 9 a further increment was observed and pK_2 could not be calculated from this data set. According to literature, the neutral form of HQ appears to a certain extent in the zwitter ionic form at the excited state when the quinoline-*N* is protonated, while the phenolic

O is deprotonated, which can lead to the formation of intramolecular hydrogen bonding preventing the determination of the ground state protonation constant [31,32].

3.2. Stability of the Ga(III)-hydroxypyrone and -hydroxythiopyrone complexes

The complex formation processes of the hydroxy(thio)pyrone ligands with Ga(III) were studied primarily by pH-potentiometry in aqueous solution. Lower ligand concentrations had to be applied for the thio derivatives due to their limited water solubility. The stoichiometries of the metal complexes and the cumulative stability constants furnishing the best fits to the experimental data are listed in Table 3.

Table 3

In all the $[GaL]^{2+}$, $[GaL_2]^{+}$ and $[GaL_3]$ complexes formed the bidentate (O,O) or (O,S) coordination modes are the most feasible. Since the coordination of maltol and allomaltol to the metal ion starts already at pH < 2, the overall formation constants of the *mono*-ligand complexes formed at low pH were determined by UV-Vis spectrophotometry on individual samples following the changes of the ligand bands (see Fig. S3), where KCl was partially or completely replaced by HCl in order to adjust the pH and keep the ionic strength constant. By fitting the spectra recorded between pH 1.0 and 2.0 the stability constants for $[GaL]^{2+}$ complexes could be calculated. After keeping them constant, the logβ values of the *bis* and *tris*-ligand species were determined by pH-potentiometry. The UV−Vis spectra of the Ga(III)/hydroxy(thio)pyrone ligand systems revealed that λ_{max} is situated between those of the completely protonated and deprotonated forms of the metal-free ligands in the pH-range of the complex formation. The bands belonging to the complexes were relatively well-separated in the case of the (O,O) donor ligands and λ_{max} at 306 and 292 nm was found for the maltol and allomaltol species, respectively (*c.f.* data of metal-free ligands in Table 1). This feature allowed determining the stability constants of the Ga(III) complexes of maltol and allomaltol

from the UV spectrophotometric titration data (Table 3), which are in a good agreement with the pH-potentiometric results. However, the speciation was also supported by the UV−Vis spectra recorded for the hydroxythiopyrone complexes (Fig. 3) via the changes of the absorbance values at 388 nm with increasing pH. At 388 nm, the absorbance is higher in the acidic pH range where the various Ga(III) complexes are formed. This is based on the stability constants calculated from the pH-potentiometric data, as compared with the values obtained in the absence of the metal ion. At higher pH, however, identical spectra with those of the metal-free ligand were observed owing to complex dissociation.

Fig. 3

Furthermore, the effect of the composition of the background electrolyte on the complex formation of Ga(III) with maltol was studied by replacing chloride with nitrate (Table 3). The collected data reveal similar stability constants as expected considering the quite low stability of Ga(III)-chlorido complexes [33]. Therefore the presence of chloride instead of nitrate ions has no measurable influence on the stabilities.

^{1}H NMR spectroscopy was found to be an adequate method to confirm the speciation in aqueous solution of these Ga(III) complexes. First of all slow ligand-exchange processes were seen with respect to the NMR time scale as the chemical shifts of the protons of the free and Ga-bound ligand were observed separately (Fig. 4). The complex formation is accompanied by significant electronic shielding effects, namely downfield shifts of all the aromatic ring and methyl protons are observed in all cases (Fig. 5a and Table S1) as it was also found previously in the case of the *tris*(maltolato) [34] and *tris*(thiomaltolato) complexes [23].

Figs. 4 and 5

Furthermore, the signals of the *mono*, *bis* and *tris*-ligand complexes could be distinguished well (for maltol see Fig. S4). It is noteworthy that the [GaL_3] complex of maltol predominates

between pH 6−8 in the milimolar concentration range and complete dissociation is observed at pH > 10. Integrated areas of the signals of all corresponding protons of the pH-dependent non-bound ligand peaks and those of the complexes (non pH-dependent) are depicted in Fig. 5b together with the summed concentration distribution curves calculated on the basis of the stability constants. The strong correlation between the data of the two independent methods supports the accuracy of the stability constants determined. Octahedral coordination compounds of bidentate and unsymmetrical ligands in the *tris*-ligand complexes can exist in geometric meridional (*mer*) or facial (*fac*) isomers. The X-ray structure of the maltolato complex [GaL_3] reveals the formation of the *mer* isomer [2], while the thiomaltolato complex exists exclusively in the *fac* geometry with a three-fold symmetry axis in solid state [23], or at least these forms are crystallized out from the solution easier. The maltolato complex is known to undergo very rapid isomerization in solution [34], however significant line broadening was not observed in the ^{1}H NMR spectra (Figs. 4, 5a), which may indicate existence of merely one kind if isomer under the applied conditions. Similar behavior was observed for *tris*(allomaltolato)gallium complex (Fig. 4). The ^{1}H NMR spectrum of the *tris*(thiomaltolato)gallium species were recorded in d_6-DMSO and featured such sharp peaks suggesting that *fac* geometry is the most probable in this solvent [23]. The complex does not seem to dissociate under these conditions as no free ligand was observed [23]. The situation is clearly different in purely aqueous solution. Considerable amounts of non-bound ligand were detected at physiological pH due to partial dissociation of the complex [GaL_3], which was expected based on the stability constants. On the other hand, two sets of peaks belonging to the *tris*-ligand metal complexes appear in the spectra of the Ga−hydroxythiopyrone systems (Fig. 4). This is most probably a consequence of isomerization, which is relatively slow on the NMR time scale. The resolution of the peaks of the methyl protons in the range of 2.4−2.7

ppm in the Ga(III)−thiomaltol system allows concluding that the peak of the *mer* isomer with three non-equivalent methyl groups is found upfield to that of the *fac* isomer (Fig. 4).

The stability constants of the Ga(III)−hydroxy(thio)pyrone complexes (Table 3) show the following order: thioallomaltol < thiomaltol < allomaltol < maltol. The exchange of oxygen to sulfur in the hydroxypyrone molecule undoubtedly results in a decrease in the stability as it was also found with respect to the Fe(III)−thiomaltolato and –maltolato complexes [35]. The position of the ring methyl group has also a distinct influence on the speciation, namely the complexes of the allo derivatives are less stable. It is also important to note that in these systems always the *tris*-ligand complexes predominate at physiological pH. It can be concluded that the stability of the Ga(III)–maltolato and –thiomaltolato complexes are comparable to that of Fe(III) [34,35], and both metal ions form more stable complexes with the (O,O) donor maltol. This is in accordance with Pearson's principle [36] *i.e.* both metal ions are considered as hard Lewis acids.

3.3. Stability of the Ga(III)-8-hydroxyquinoline complexes

The low aqueous solubility of the neutral Ga(III)−HQ complex hindered the application of pH-potentiometry for stability constant determination in water, since at least ~1 mM concentrations are required for this method and at maximum c_L ~0.05 mM at 1:3 metal-to-ligand ratio could be used without precipitation. Therefore, complexation was studied by pH-potentiometry in 30% and 60% (w/w) DMSO/H_2O solvent mixtures and the resulting overall stability constants are shown in Table 4.

Table 4

Logβ values of the *mono*-ligand complexes were determined by UV-Vis spectrophotometry at pH 1–2 using the batch procedure already described for the maltolato and allomaltolato complexes (*vide supra*). Similar experiments were reported earlier, using a 50% 1,4-

dioxane/H_2O mixture and somewhat lower constants were published [37] than obtained in 60% DMSO/H_2O. In order to determine the stability of the Ga(III)−HQ complexes in water, the complex formation of the reference compound HQS was studied under the same conditions (in 30% and 60% (w/w) DMSO/H_2O). In addition, pH-potentiometry was used in pure water due the much higher water solubility of HQS and the data obtained are in good agreement with literature values [29]. For comparison, the logβ values of the Ga(III)−maltolato species were also determined under the same conditions (see constants in Table 4). These experiments reveal increasing overall stability constants for HQS and maltol species with increasing DMSO content, thus with increasing $1/\varepsilon_r$ values (see Fig. S5). Logβ values of the Ga(III)−HQ *mono*, *bis* and *tris*-ligand complexes in pure aqueous phase were extrapolated from the values obtained in the DMSO/H_2O mixtures with the slopes of the linear curves of HQ and that of the structurally similar HQS (Table 4). It is obvious that both HQ and HQS coordinate to the Ga(III) ion in their complexes in a bidentate way via their (N,O) donor sets [1,28].

Spectroscopic titrations were also done in highly diluted solution of the Ga(III)−HQ system (c_{HQ} = 50 μM) in water. The determination of the stability constants by UV-Vis spectrophotometric titrations was performed as for the hydroxypyrones (see constants in Table 4 and spectra in Fig. S6), but a longer light path was used to reach adequate absorbance values. The application of fluorimetry to determine stability constants of metal complexes is fairly rare in the literature [16], although it may be an absolutely beneficial method in the case of poorly water-soluble fluorescent compounds. The fluorogenic property of HQ in which the fluorescence intensity is enhanced by the coordination of Ga(III) (or Al(III)) is well known [6]. HQ is weakly fluorescent (*vide supra*) but when the ligand is bound to Ga(III) the intensity of the light emission was ten-times stronger. A representative 3-dimensional fluorescence spectrum of the Ga(III)−HQ system at physiological pH is shown in Fig. 6a.

Fig. 6

This feature allowed us to monitor the cellular accumulation and distribution of *tris*(8-hydroxyquinolinato)gallium in living human cancer cells by fluorescence microscopy (*vide infra*) and determination of stability constants of complexes formed as well. Fluorescence titration curves recorded at various metal-to-ligand ratios were analyzed (Fig. 6b,c) and the logβ values were calculated from the spectral changes with the PSEQUAD program [18] (Table 4). The stability constants of the Ga(III)-HQ complexes obtained by the spectroscopic methods are in a good agreement and are reasonably similar to the values estimated from the data obtained in DMSO/water mixtures. Based on the stability constants, the negative logarithm of the equilibrium concentrations of the free metal ion at pH 7.40 (pM, c_{Ga} = 1 μM, Ga:L = 1:10) were calculated as 21.0 and 20.7 for HQ and HQS, respectively, showing the similar Ga(III) binding ability of these compounds. The concentration distribution curves of the Ga(III)-HQ system (Fig. 7) support the predominant formation of *tris*(8-hydroxyquinolinato)gallium at physiological pH.

Fig. 7

3.4. Comparison of tris(maltolato)gallium and tris(8-hydroxyquinolinato)gallium complexes

The stoichiometry and stability of the Ga(III)-containing clinically tested drug candidates are especially important under biologically relevant conditions in aqueous phase. This information is relevant to elucidate the pharmacokinetic properties of a drug candidate and is an important contribution to the prediction of its fate in the human body, especially in blood serum. Therefore, the distribution of the *tris*-ligand Ga complexes of maltol and HQ was calculated based on the stability constants (Table 4) at physiological pH at various total concentrations and depicted in Fig. 8. In both cases, the predominant complexes are the [GaL_3] species under the applied conditions and, as expected, the partial dissociation resulting

in free ligand and $[Ga(OH)_4]^-$ is more pronounced with decreasing total concentrations. Undoubtedly, *tris*(8-hydroxyquinolinato)gallium is able to preserve the original entity harder owing to its prominent high stability as the extent of complex dissociation is much lower at a given concentration compared with the maltolato compound. Therefore, the coordinating ligand in the maltolato complex is supposed to be exchanged partly or completely more easily by endogenous bioligands, such as human serum transferrin, than in the 8-hydroxyquinolinato complex. This property may lead to significantly different biodistribution processes once administered to a living organism.

Fig. 8

3.5. Fluorescence monitoring of cellular distribution of tris(8-hydroxyquinolinato)gallium

The fluorescence properties of the *tris*(8-hydroxyquinolinato)gallium complex allowed monitoring cellular distribution in living SW480 colon cancer cells. Fluorescence microscopy revealed that the Ga(III)–HQ complex was stable for several hours in cellular environment, since the free ligands exhibit markedly lower fluorescence intensity. SW480 cells were incubated with 150 or 300 μM the Ga(III)−HQ complex for 5 and 30 min as well as 1 and 3 h. Brightfield images of treated cells were taken prior to fluorescence imaging to determine the viable state of the cells. After 3 h of incubation with 150 μM of the Ga(III)−HQ complex, cells were strongly affected and changes in morphology were observed. However, the Ga(III)−HQ complex was visualized in living cells (Fig. 9), and was found to accumulate within minutes in the cytoplasm, whereas no uptake into the nucleus was observed. In the cytoplasm the Ga(III)−HQ complex showed a striking affinity to a mesh-like structure that surrounds the nucleus. This finding may suggest a co-localization with the endoplasmic reticulum (ER) or ER-associated proteins however; it should be proved by further studies.

Fig. 9

4. Conclusions

Solution equilibrium studies in aqueous phase on the Ga(III) complexes of HQ, HQS and various hydroxy(thio)pyrones were performed by a combined potentiometric and spectroscopic approach and revealed the formation of *mono*, *bis* and *tris*-ligand metal complex species for all ligands. Complexes of the general formula $[GaL_3]$ predominate at physiological pH, but dissociation can take place at the higher basic pH range, due to the strong tendency of the Ga(III) ion to hydrolyze. The ability of the ligands to prevent the metal ion from hydrolysis depends on their Ga(III) binding ability, which shows the following order: thioallomaltol < thiomaltol < allomaltol < maltol << HQS ~ HQ. As the *tris*(8-hydroxyquinolinato)gallium(III) complex possesses an *ca.* 8 orders of magnitude higher stability constant than *tris*(maltolato)gallium(III), it is able to preserve its original composition without high extent of complex dissociation at very low concentrations, as found in biological systems. This may have an impact on the biodistribution of these antitumor compounds. It was also shown that the *tris*-hydroxythiopyrone complexes can undergo fast isomerization in aqueous solution resulting in the coexistence of the *fac* and *mer* isomers. Fluorescence spectroscopy was found to be an efficient tool for the determination of the stability constants of the Ga(III)−HQ complexes, which have fairly low water solubility. On the other hand, the uptake and intracellular localization of the fluorescent complex *tris*(8-hydroxyquinolinato)gallium(III) could be followed by fluorescence microscopy in living cells for several hours. Moreover, this technique allowed us to visualize the intracellular distribution of the compound, which is relevant for further cell biological mode-of-action studies.

Supplementary data

The supporting information contains figures featuring pH-dependent UV-Vis, fluorescence and ^{1}H NMR spectra and correlation diagrams.

5. Abbreviations

allomaltol	5-hydroxy-2-methyl-4H-pyran-4-one
allothiomaltol	5-hydroxy-2-methyl-4-thiopyrone
D	distribution coefficient
ε_r	relative permittivity (or dielectric constant)
ER	endoplasmic reticulum
fac	facial
HQ	8-hydroxyquinoline, oxine
HQS	8-hydroxyquinoline-5-sulfonate, sulfoxine
KP46	*tris*(8-quinolinolato)Ga(III)
λ_{EM}	fluorescence emission wavelength
λ_{EX}	fluorescence excitation wavelength
maltol	3-hydroxy-2-methyl-4H-pyran-4-one
MEM	Minimal Essential Medium
mer	meridional
P	partition coefficient
PBS	phosphate buffered saline
thiomaltol	3-hydroxy-2-methyl-4-thiopyrone

Acknowledgments

This work has been supported by the Hungarian Research Foundation OTKA 103905, Hungarian-Austrian Action Fund (84öu1). É.A. Enyedy gratefully acknowledges the financial support of J. Bolyai research fellowship.

References

[1] M.A. Jakupec, B.K. Keppler, Curr. Top. Med. Chem. 4 (2004) 1575–1583.

[2] L.R. Bernstein, T. Tanner, C. Godfrey, B. Noll, Metal-Based Drugs 7 (2000) 33–47.

[3] P. Collery, B.K. Keppler, C. Madoulet, B. Desoize, Crit. Rev. Oncol. Hematol. 42 (2002) 283–296.

[4] M.A. Jakupec, M. Galanski, V.B. Arion, G.C. Hartinger, B.K. Keppler, J. Chem. Soc., Dalton Trans. (2008) 183–194.

[5] L.R. Bernstein, in: Metallotherapeutic Drugs and Metal-Based Diagnostic Agents: The Use of Metals in Medicine (Eds. M. Gielen, B.R.T. Tiekink) vol. 14, John Wiley & Sons, Ltd, 2005 259–277.

[6] F. Zhang, X. Liu, F. Huang, Z. Zhuo, L. Lu, Z. Xu, Y. Wang, X. Tao, W. Bian, W. Tang, Chinese Science Bulletin 56 (2011) 479–483.

[7] C.R. Chitambar, D.P. Purpi, J. Woodliff, M. Yang, J.P. Wereley, J. Pharmacol. Exp. Ther. 322 (2007) 1228–1236.

[8] L.R. Bernstein, J.J.M. van der Hoeven, R.O. Boer, Anticancer Agents Med. Chem. 11 (2011) 585–590.

[9] J. Narasimhan, W.E. Antholine, C.R. Chitambar, Biochem. Pharmacol. 44 (1992) 2403–2408.

[10] M. Groessl, A. Bytzek, C.G. Hartinger, Electrophoresis 30 (2009) 2720–2727.

[11] A.V. Rudnev, L.S. Foteeva, C. Kowol, R. Berger, M.A. Jakupec, V.B. Arion, A.R. Timerbaev, B.K. Keppler, J. Inorg. Biochem. 100 (2006) 1819–1826.

[12] Z. D. Liu, H. H. Khodr, D. Y. Liu, S. L. Lu, R. C. Hider, J. Med. Chem. 42 (1999) 4814–4823.

[13] W. Kandioller, C.G. Hartinger, A.A. Nazarov, M.L. Kuznetsov, R.O. John, C. Bartel, M.A. Jakupec, V.B. Arion, B.K. Keppler, Organometallics 28 (2009) 4249–4251.

[14] G. Gran, Acta Chem. Scand. 4 (1950) 559−577.

[15] H.M. Irving, M.G. Miles, L.D. Pettit, Anal. Chim. Acta 38 (1967) 475−488.

[16] SCQuery, The IUPAC Stability Constants Database, Academic Software (Version 5.5), Royal Society of Chemistry, 1993−2005.

[17] P. Gans, A. Sabatini, A. Vacca, Talanta 43 (1996) 1739−1753.

[18] L. Zékány, I. Nagypál, in: Computational Methods for the Determination of Stability Constants (Ed.: D. L. Leggett), Plenum Press, New York, 1985, pp. 291−353.

[19] E. Farkas, E. Kozma, T. Kiss, I. Toth, B. Kurzak, J. Chem. Soc. Dalton Trans. (1995) 477−481.

[20] S.K. Poole, C.F. Poole, J. Chromatogr. B 797 (2003) 3−19.

[21] É.A. Enyedy, D. Hollender , T. Kiss, J. Pharmaceut. Biomed. Anal. 54 (2011) 1073−1081.

[22] É.A. Enyedy, L. Horváth, K. Gajda-Schrantz, G. Galbács, T. Kiss, J. Inorg. Biochem. 100 (2006) 1936−1945.

[23] V. Monga, B.O. Patrick, C. Orvig, Inorg. Chem. 44 (2005) 2666−2677.

[24] B. Song, K. Saatchi, G.H. Rawji, C. Orvig, Inorg. Chim. Acta 339 (2002) 393−399.

[25] B. L. Ellis, A.K. Duhme, R.C. Hider, M.B. Hossain, S. Rizvi, D. van der Helm, J. Med. Chem. 39 (1996) 3659−3670.

[26] S. Chaves, R. Jelic, C. Mendonca, M. Carrasco, Y. Yoshikawa, H. Sakurai, M.A. Santos, Metallomics 2 (2010) 220–227.

[27] S. Tsakovski, K. Benkhedda, E. Ivanova, F.C. Adams, Anal. Chim. Acta 453 (2002) 143−154.

[28] P. Letkeman, A.E. Martell, R.J. Motekaitis, J. Coord. Chem. 10 (1980) 47–53.

[29] O. Jarjayes, S. Hamman, F. Sarrazin, T. Benaissa, C.G. Beguin, New J. Chem. 22 (1998) 361–366.

[30] M. Born, Z. Phys., 1 (1920) 45–48.

[31] E.M. Filip, I.V. Humelnicu, C.I. Ghirvu, Acta Chemica Iasi, 17 (2009) 85–96.

[32] M. Amati, S. Belviso, P.L. Cristinziano, C. Minichino, F. Lelj, I. Aiello, M. La Deda, M. Ghedini, J. Phys. Chem. A 111 (2007) 13403–13414.

[33] M.H. Mihalov, Polyhedron, 36 (1974) 107–113.

[34] M.M. Finnegan, T.G. Lutz, W.O. Nelson, A. Smith, C. Orvig, Inorg. Chem. 26 (1987) 2171−2176.

[35] S. Chaves, S. Canario, M.P. Carrasco, L. Mira, M.A. Santos, J. Inorg. Biochem. 114 (2012) 38–46.

[36] R.G. Pearson, J. Am. Chem. Soc. 85 (1963) 3533–3539.

[37] M. Thompson, Anal. Chim. Acta, 98 (1976) 357–363.

Legends to Figures/Charts

Chart 1 Chemical structures of the ligands

Fig. 1 UV-Vis absorption spectra of allomaltol (a) and thiomaltol (b) recorded at different pH values (2−11.5). The insets show the concentration distribution curves for ligand species with the pH-dependence of absorbance values at 308 nm and 388 nm (×), respectively. {$c_{allomaltol}$ = *102 μM;* $c_{thiomaltol}$ = *52 μM; l = 1 cm; t = 25.0 °C, I = 0.20 M (KCl)}.*

Fig. 2 UV-Vis absorption spectra of HQ recorded at different pH values (2−11.5). The inset shows the molar absorption spectra of the individual ligand species (H_2L^+, HL, L^-). {c_{HQ} = *50 μM; l = 2 cm; t = 25.0 °C, I = 0.20 M (KCl) in aqueous phase}.*

Fig. 3 Concentration distribution curves of the Ga(III)–thiomaltol system and the pH-dependence of the absorbance at 388 nm for the Ga species (×) and the ligand (●) {$c_{thiomaltol}$ = *102 μM;* M:L = 1:3*; l = 1 cm; t = 25.0 °C, I = 0.20 M (KCl)}.*

Fig. 4 ^{1}H NMR spectra of Ga(III)/hydroxy(thio)pyrone systems recorded at pH 7.0 for maltol and allomaltol and at pH 7.4 for thiomaltol and thioallomaltol. The peaks of the free ligand are highlighted in grey. {c_L = *3 mM (hydroxypyrones); 1 mM (hydroxythiopyrones);* M:L = 1:3*; t = 25.0 °C, I = 0.20 M (KCl), 10% D_2O}.*

Fig. 5 ^{1}H NMR spectra of the Ga(III)–maltol system recorded at various pH values. (a) Summed concentration distribution curves for the Ga-bound (black line) and free ligand (grey line) species in the Ga(III)–maltol system calculated on the basis of the stability constants and

^{1}H NMR peak integrals: bound (×) and free (●) ligand. (b) {c_{maltol} = *3 mM;* M:L = 1:3*; t = 25.0 ˚C, I = 0.20 M (KCl), 10% D_2O}.

Fig. 6 The 3-dimensional fluorescence spectrum of the Ga(III)–HQ (1:3) system at pH 7.4 in water (a) and its pH-dependent fluorescence spectra at 367 nm excitation (b). pH-dependent fluorescence emission intensities at 533 nm of HQ (×), and the Ga(III)–HQ system at metal-to-ligand ratios of 1:3 (●), 1:5 (◊), 1:2 (Δ), 1:1 (○) (c). *{λ_{EX} = 367 nm; c_{HQ} = 50 μM; t = 25.0 ˚C, I = 0.20 M (KCl)}.*

Fig. 7 Concentration distribution curves of the Ga(III)–HQ (1:3) system. {c_{HQ} *= 50 μM; M:L = 1:3; t = 25.0 ˚C, I = 0.20 M (KCl)}.*

Fig. 8 Representative concentration distribution diagram for *tris*(8-hydroxyquinolinato)gallium (black lines) and *tris*(maltolato)gallium (grey lines) at various total concentrations and physiological pH. The dashed line shows the concentration range where the complex is not water soluble. *{$c_{[GaL3]}$ = 1-300 μM; t = 25.0 ˚C, I = 0.20 M (KCl)}.*

Fig. 9 Time dependent live-cell fluorescence microscopy images (upper row) and corresponding brightfield images (lower row) from SW480 colon carcinoma cells treated with 150 μM Ga(III)–HQ. The scale bar represents 20 μm.

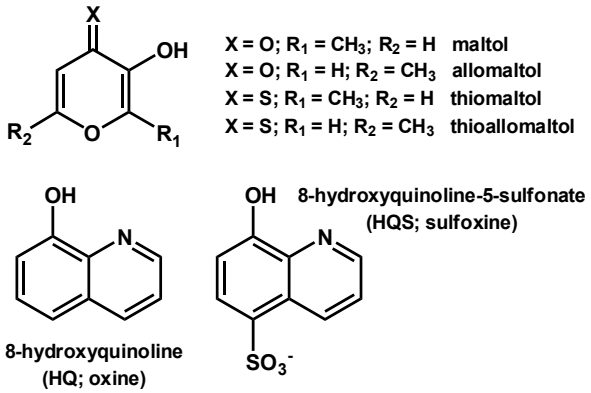
X
OH
R2
O
R1
X = O; R1 = CH3; R2 = H maltol
X = O; R1 = H; R2 = CH3 allomaltol
X = S; R1 = CH3; R2 = H thiomaltol
X = S; R1 = H; R2 = CH3 thioallomaltol
OH
N
8-hydroxyquinoline
(HQ; oxine)
OH
N
SO3-
8-hydroxyquinoline-5-sulfonate
(HQS; sulfoxine)

Chart 1

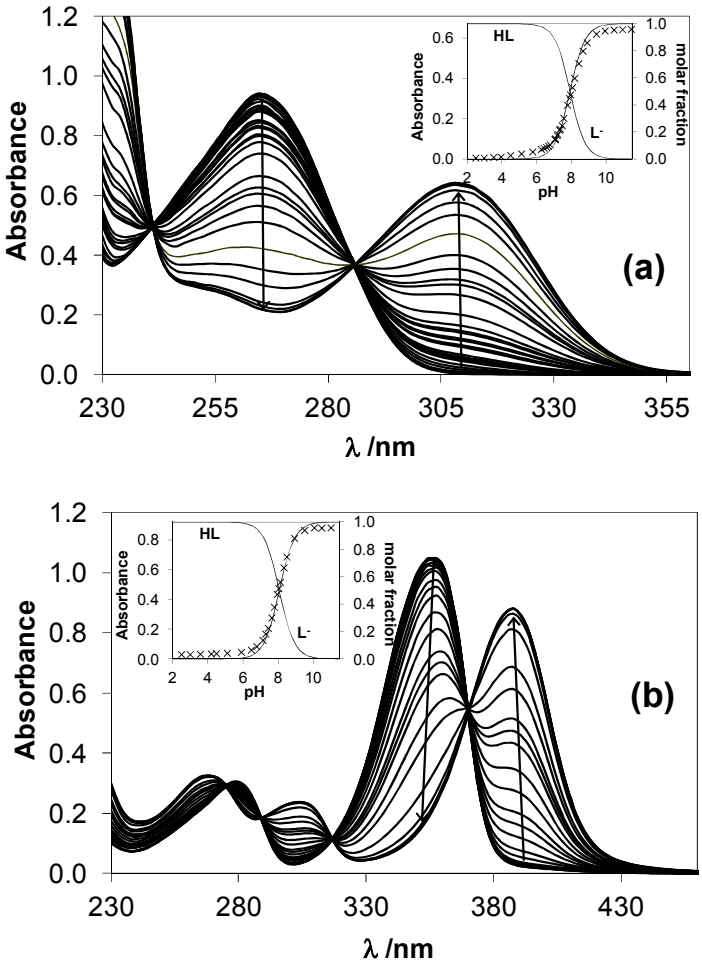

Fig. 1

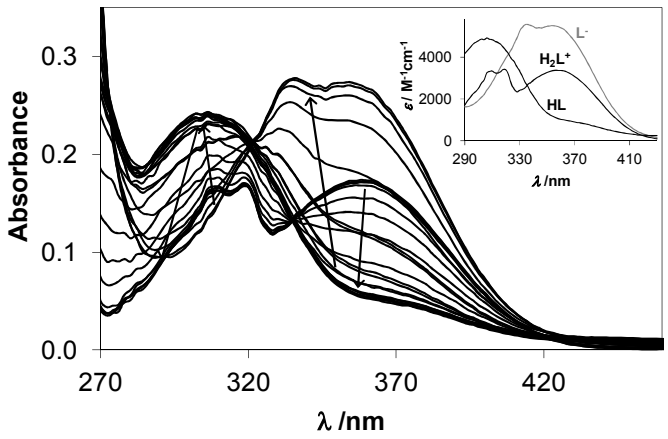
Absorbance
0.3
0.2
0.1
0.0
270
320
370
420
λ /nm
ε / M-1cm-1
4000
2000
0
290
330
370
410
λ /nm
L-
H2L+
HL

Fig. 2

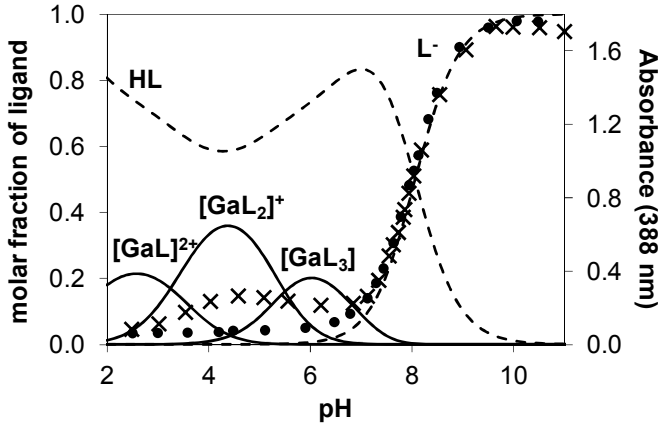
molar fraction of ligand
1.0
0.8
0.6
0.4
0.2
0.0
HL
[GaL2]+
[GaL]2+
[GaL3]
L-
2
4
6
8
10
pH
Absorbance (388 nm)
1.6
1.2
0.8
0.4
0.0

Fig. 3

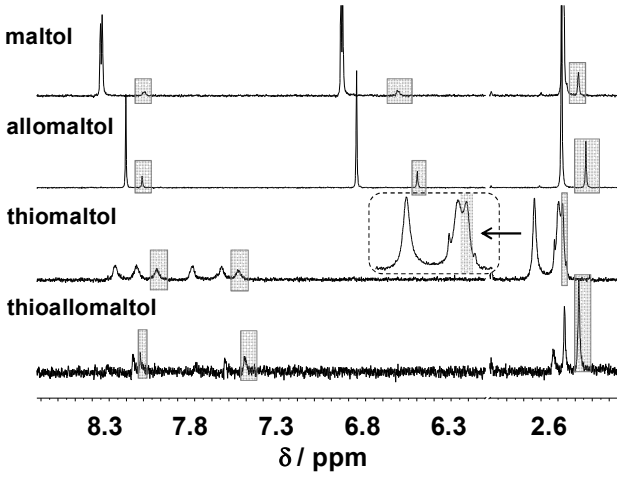
maltol
allomaltol
thiomaltol
thioallomaltol
8.3
7.8
7.3
6.8
6.3
2.6
δ / ppm

Fig. 4

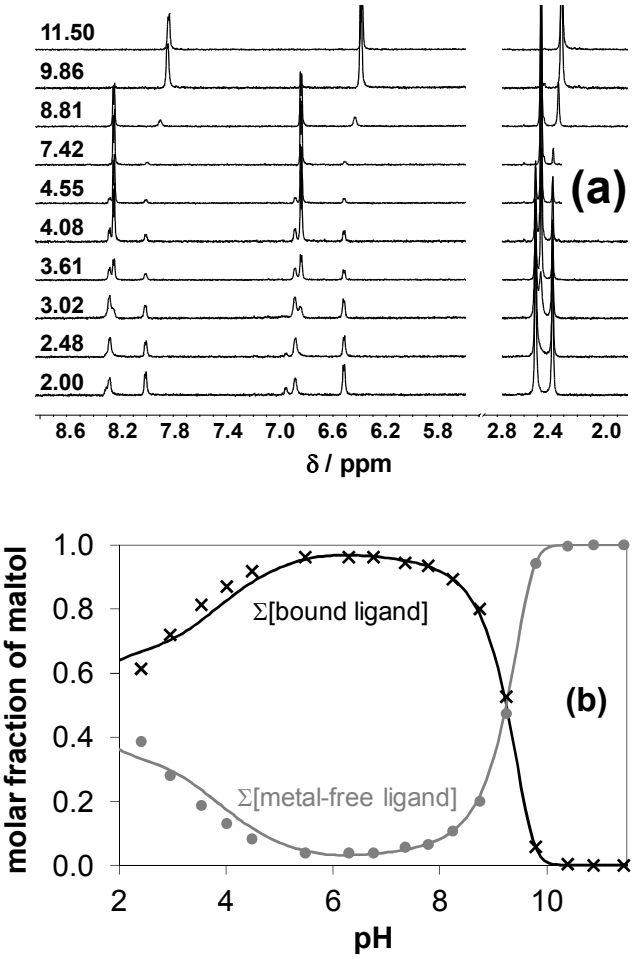
11.50
9.86
8.81
7.42
4.55
4.08
3.61
3.02
2.48
2.00
(a)
8.6 8.2 7.8 7.4 7.0 6.6 6.2 5.8
2.8 2.4 2.0
δ / ppm
molar fraction of maltol
1.0
0.8
0.6
0.4
0.2
0.0
Σ[bound ligand]
Σ[metal-free ligand]
(b)
2 4 6 8 10
pH

Fig. 5

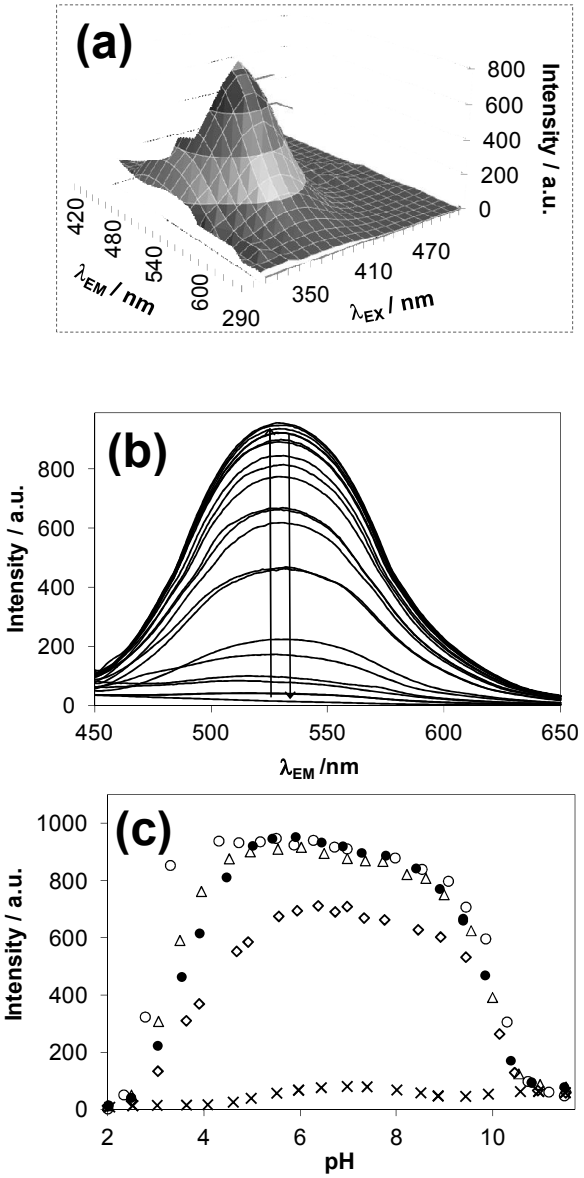
(a)
Intensity / a.u.
800
600
400
200
0
420
480
540
600
λEM / nm
290
350
410
470
λEX / nm
(b)
Intensity / a.u.
800
600
400
200
0
450
500
550
600
650
λEM /nm
(c)
Intensity / a.u.
1000
800
600
400
200
0
2
4
6
8
10
pH

Fig. 6

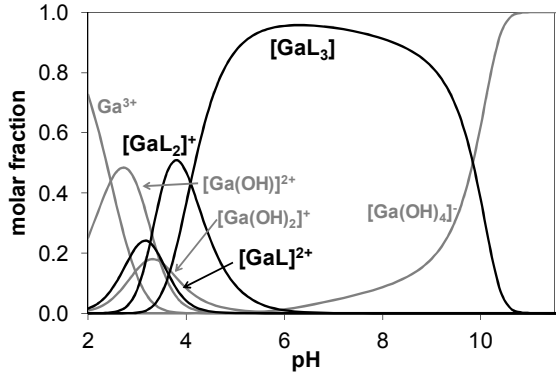
1.0
0.8
0.6
0.4
0.2
0.0
molar fraction
Ga3+
[GaL2]+
[Ga(OH)]2+
[Ga(OH)2]+
[GaL]2+
[GaL3]
[Ga(OH)4]-
2
4
6
8
10
pH

Fig. 7

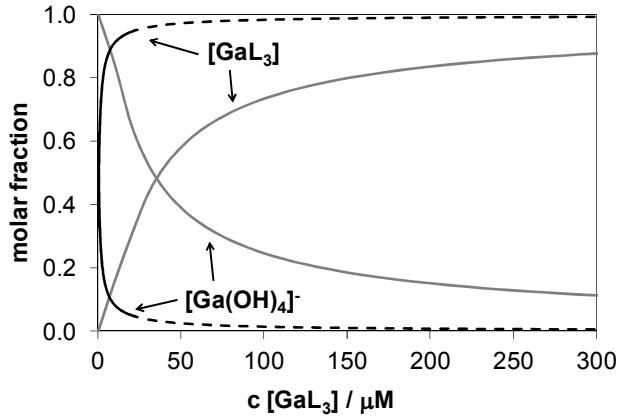
1.0
0.8
0.6
0.4
0.2
0.0
molar fraction
[GaL3]
[Ga(OH)4]-
0
50
100
150
200
250
300
c [GaL3] / μM

Fig. 8

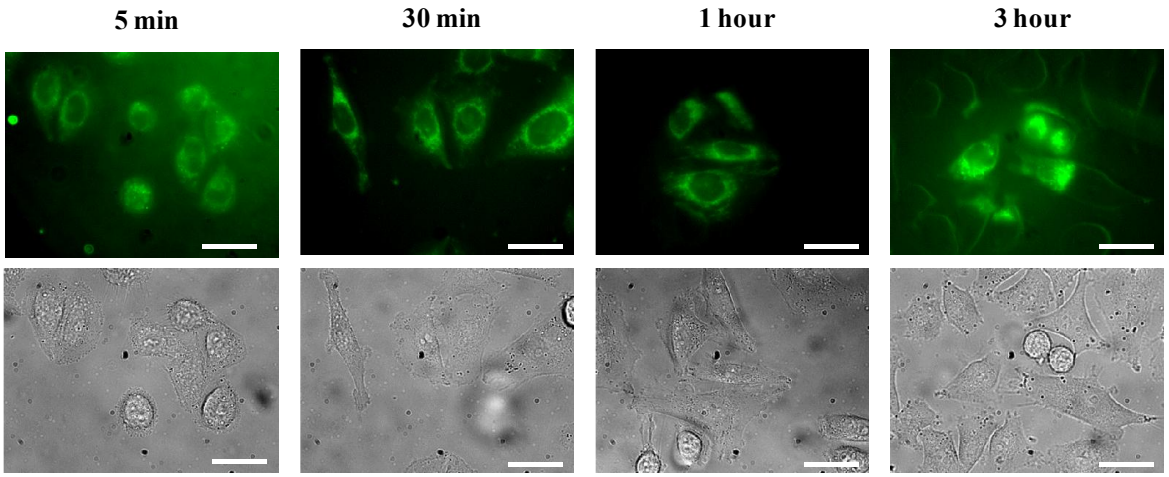

Fig. 9

Table 1

Proton dissociation constants (pK_a) of the hydroxypyrone and hydroxythiopyrone ligands determined by pH-potentiometry and UV-Vis spectrophotometry; λ_{max} (nm) and molar absorptivity ($M^{-1}cm^{-1}$) values for the ligand species (HL, L^-) determined by UV-Vis spectrophotometric titrations; distribution and partition coefficients {t = 25 °C; I = 0.20 M (KCl)}[a]

	maltol	**allomaltol**	**thiomaltol**	**thioallomaltol**
pH-metry	8.45(1)[b]	7.97(1)	8.06(1)	7.64(1)
UV-Vis	8.46(1)	7.93(1)	8.06(1)	7.63(1)
HL	274 (8180)	264 (9150)	280 (5870)	282 (6140)
			356 (20600)	350 (20040)
$\mathbf{L^-}$	320 (7900)	308 (6190)	268 (6410)	266 (5210)
			304 (4723)	312 (7160)
			386 (17520)	378 (16560)
log$D_{7.4}$	+0.10[c]	−0.19(2)	+1.36[d]	+0.97[d]
log$P$	+0.13[c]	−0.09	+1.45(3)	+1.17(3)

[a] Standard deviations (SD) in parenthesis, values determined in pure aqueous phase.
[b] pK = 8.46(1) determined by pH-potentiometry at I = 0.20 M (KNO_3).
[c] Data taken from Ref. [21].
[d] P or $D_{7.4}$ values calculated with the equation: $D = P/(1+K_a/[H^+])$ [21]. log$P$ is equal to log $D_{2.0}$ in the case of thiomaltol and thioallomaltol.

Table 2

Proton dissociation constants (pK_a) of HQ, HQS and maltol determined by pH-potentiometry in water and at various DMSO contents {t = 25 °C}[a]

	0% (w/w)	**30% (w/w)**	**60% (w/w)**
HQ pK_1[b]	4.99(2)	4.42(1)	3.64(1)
HQ pK_2[b]	9.51(1)	10.15(1)	11.14(1)
HQS pK_1	3.90(2)	3.43(2)	2.91(1)
HQS pK_2	8.37(1)	8.91(1)	9.95(1)
maltol pK_a	8.45(1)	9.00(1)	9.87(1)

[a] Standard deviations (SD) in parenthesis; I = 0.20 M (KCl) in pure aqueous phase; I = 0.10 M (KCl) in 30% and 60% (w/w) DMSO/H_2O.

[b] From the UV-Vis titrations in pure aqueous solution: pK_1 = 4.95(1); pK_2 ~ 9.75(5); $\lambda_{max}/\varepsilon$ ($M^{-1}cm^{-1}$) values: 308 nm(3320), 318 nm (3420), 358 nm (3370) for H_2L^+; 306 nm (4914) for HL; 334 nm (5560), 354 nm (~5500) for L^-. From the fluorimetric titrations in pure aqueous solution: pK_1 = 4.96(1)

Table 3

Overall stability constants (logβ) of the Ga(III) complexes of hydroxypyrone and hydroxythiopyrone ligands determined by pH-potentiometry in aqueous solution {t = 25 °C; I = 0.20 M (KCl)}[a]

	maltol[b]	**allomaltol**[c]	**thiomaltol**	**thioallomaltol**
logβ[GaL]$^{2+}$	10.63(2)[d]	9.86(1)[d]	10.37(6)	9.63(5)
logβ[GaL$_2$]$^{+}$	21.07(4)	19.23(2)	19.05(6)	17.67(6)
logβ[GaL$_3$]	28.77(2)	26.87(1)	25.59(2)	24.71(5)
fitting parameter (mL)	3.89×10^{-3}	2.31×10^{-3}	1.62×10^{-3}	4.25×10^{-3}

[a] Standard deviations (SD) in parenthesis, values determined in pure aqueous phase.
[b] UV titrations: logβ[GaL$_2$]$^{+}$ = 20.66(6); logβ[GaL$_3$] = 28.76(4). Constants at I = 0.20 M (KNO_3): logβ[GaL]$^{2+}$ = 10.53(5); logβ[GaL$_2$]$^{+}$ = 21.03(3); logβ[GaL$_3$] = 28.73(2).
[c] UV titrations: logβ[GaL$_2$]$^{+}$ = 19.13(3); logβ[GaL$_3$] = 26.98(1).
[d] Determined by UV spectrophotometric measurements at pH 1-2.

Table 4

Overall stability constants (logβ) of the Ga(III) complexes of HQ, HQS and maltol determined by pH-potentiometry under various conditions $\{t = 25\ °C\}$[a]

		0% (w/w)	30% (w/w)	60% (w/w)
HQ	**logβ[GaL]$^{2+}$**	13.13(8)[b]	13.64(6)[c]	14.50(5)[c]
		13.04[d]		
	logβ[GaL$_2$]$^{+}$	25.54(5)[e]	26.60(3)	30.15(2)
		25.58(3)[b]		
		25.73[d]		
	logβ[GaL$_3$]	36.79(1)[e]	37.87(2)	41.93(3)
		36.41(1)[b]		
		36.61[d]		
	fitting parameter (mL)	–	5.99×10^{-3}	3.89×10^{-3}
HQS	**logβ[GaL]$^{+}$**	11.99(1)[c]	12.63(3)[c]	14.13(5)[c]
	logβ[GaL$_2$]$^{-}$	23.25(2)	25.01(2)	27.14(9)
	logβ[GaL$_3$]$^{3-}$	33.17(1)	35.06(1)	38.36(9)
	fitting parameter (mL)	2.16×10^{-3}	2.43×10^{-3}	7.35×10^{-3}
maltol	**logβ[GaL]$^{2+}$**	10.63(2)[c]	11.33(1)[c]	12.15(2)[c]
	logβ[GaL$_2$]$^{+}$	21.07(4)	22.24(3)	24.74(6)
	logβ[GaL$_3$]	28.77(2)	30.64(1)	34.08(4)
	fitting parameter (mL)	3.89×10^{-3}	5.06×10^{-3}	8.53×10^{-3}

[a] Standard deviations (SD) in parenthesis; I = 0.20 M (KCl) in pure aqueous phase; I = 0.10 M (KCl) in 30% and 60% (w/w) DMSO/H_2O.
[b] Determined by UV-Vis spectrophotometric titrations (pH > 2).
[c] Determined by UV-Vis spectrophotometric measurements (pH 1-2).
[d] Estimated from the logβ values of HQ complexes measured in 30% and 60% (w/w) DMSO mixtures the with the help of the slopes of the logβ *vs.* $1/\varepsilon_r$ curves of Ga(III) complexes of HQS and HQ
[e] Determined by spectrofluorimetric titrations (pH > 2).